Faraday Discussions

Accepted Manuscript

This manuscript will be presented and discussed at a forthcoming Faraday Discussion meeting. All delegates can contribute to the discussion which will be included in the final volume.

Register now to attend! Full details of all upcoming meetings: http://rsc.li/fd-upcoming-meetings

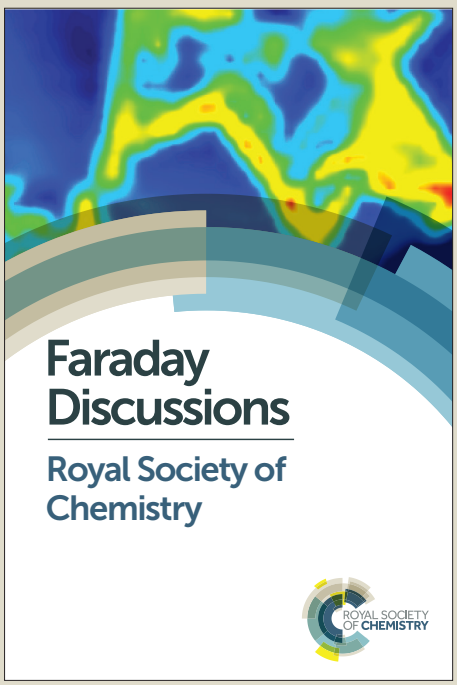

This is an *Accepted Manuscript*, which has been through the Royal Society of Chemistry peer review process and has been accepted for publication.

Accepted Manuscripts are published online shortly after acceptance, before technical editing, formatting and proof reading. Using this free service, authors can make their results available to the community, in citable form, before we publish the edited article. We will replace this *Accepted Manuscript* with the edited and formatted *Advance Article* as soon as it is available.

You can find more information about *Accepted Manuscripts* in the Information for Authors.

Please note that technical editing may introduce minor changes to the text and/or graphics, which may alter content. The journal's standard Terms & Conditions and the Ethical guidelines still apply. In no event shall the Royal Society of Chemistry be held responsible for any errors or omissions in this *Accepted Manuscript* or any consequences arising from the use of any information it contains.

ROYAL SOCIETY OF CHEMISTRY

www.rsc.org/faraday_d

Aqueous dispersions of oligomer-grafted carbon nanomaterials with controlled surface charge and minimal framework damage

Sheng Hu,[a] Shu Chen,[b] Robert Menzel,[a] Angela D. Goode,[b] Mary P. Ryan,[b] Alexandra E. Porter[b] and Milo S. P. Shaffer[a1]

[a] *Department of Chemistry and London Centre for Nanotechnology, Imperial College London, Exhibition Road, London SW7 2AZ, UK*

[b] *Department of Materials and London Centre for Nanotechnology, Imperial College London, Exhibition Road, London SW7 2AZ, UK*

[1] *Corresponding author. Department of Chemistry and London Centre for Nanotechnology, Imperial College London, Exhibition Road, London SW7 2AZ, UK. E-mail addresses: m.shaffer@imperial.ac.uk (M.S. P. Shaffer)*

Abstract

Functionalised carbon nanomaterials (CNMs), with an undamaged carbon framework and controlled physiochemical properties, are desirable for a wide range of scientific studies and commercial applications. The use of a thermochemical grafting approach provides a versatile means to functionalise both multi-walled carbon nanotubes (MWCNTs) and carbon black (CB) nanoparticles without altering their inherent structure. The functionalisation process was investigated by employing various types of grafting monomers; to improve water solubility, reagents were chosen that introduced ionic character either intrinsically or after further chemical reaction. The degree of grafting for both MWCNTs and CB ranged from 3-27 wt%, as established by thermal gravimetric analysis (TGA). Raman spectroscopy confirmed that the structural framework of the MWNTs was unaffected by the thermochemical treatment. The effectiveness of the surface modification was demonstrated by significantly improved dispersibility and stability in water, and further quantified by zeta-potential analysis. The concentration of stable, individualised, grafted MWNTs in water ranged from ~30-80 μg/mL, whereas functionalised CB (CB) in water showed improved dispersibility up to ~460 μg/mL. The successful preparation of structurally identical but differently functionalised nanoparticles panels, with high water compatibility and minimal framework damage, are useful for controlled experiments. For example, they can be used to explore the relationship between toxicological effects and specific physiochemical properties, such as surface charge and geometry.

1. Introduction

Carbon nanomaterials (CNMs), e.g., graphenes, carbon nanotubes (CNTs), and carbon black (CB) nanoparticles, have a significant place in nanoscience due to their extraordinary thermal, mechanical and electronic properties;[1] they have been proposed for an extensive range of applications including in biomedical contexts, such as photothermal therapy,[2,3] drug delivery[4,5] and bioimaging.[6,7] However, the hydrophobic nature of CNMs hinders straightforward liquid-phase dispersion, especially in aqueous media, or in a host polymeric matrix. Consequently, chemical functionalisation methods, including both covalent and non-covalent approaches, have been intensively investigated in an attempt to increase their solution stability. Improved processing and compatibility are considered crucial to fully exploit the impressive intrinsic properties.[8-10]

One of the most commonly used covalent functionalisation strategies involves aggressive oxidisation of the CNMs with strong acids, particularly mixtures of HNO_3 and H_2SO_4,[11,12] to produce highly concentrated aqueous dispersions. The carboxylic acid functional groups generated during such process allow amidation or esterification reactions to alter the surface properties of carbon materials further.[13,14] However, the oxidation process inevitably introduces defects into the carbon framework and reduces the dimensions of both CNTs and graphene (oxide),[15,16] leading to diminished properties.[17,18] In addition, the resulting CNMs are typically contaminated with oxidation debris.[19,20] Direct reaction with the carbon framework can also be achieved by using highly reactive intermediates, such as nitrenes, carbenes and ylides.[21] Unfortunately, these reactions typically involve time-consuming filtrations, expensive

reagents and the production of large amounts of liquid waste. These functionalisation routes have limited scalability and hence limited applicability to the current scale of CNMs production.

Non-covalent interactions between CNTs and organic materials are attractive since the CNTs surface can be modified without disturbing the characteristic π system.[22,23] Numerous studies have shown that non-covalent functionalisation using polymers or surfactants can effectively disperse nanotubes by utilizing multiple weak interactions such as π-π interactions, electrostatic interactions, hydrophobic-hydrophilic competition, *etc.*[21] However, the major drawback of non-covalent functionalisation lies in the lack of stability of the resulting assemblies due to the intrinsically weak interactions, and the usual need to maintain excess free surfactant (or other modifier) in the suspension.

An attractive thermochemical approach to grafting MWCNTs was reported, which takes advantage of the intrinsic defective groups on the so-called 'pristine' MWCNTs surface, as synthesised.[24] Heat treatment in vacuum or inert atmosphere generates surface radicals, suitable for further reaction. Recently, the grafting approach has been applied to the preparation of highly water-compatible MWCNTs, stabilised by cationic, anionic, or non-ionic grafted species; the thermal activation process was followed by 'grafting from' polymerisations, and hydrophilising post-functionalisation reactions on the initially non-ionic monomers.[25] In contrast to traditional acid oxidation protocols, the thermochemical method has significant advantages of minimising the damage to the nanotube framework, whilst avoiding production of debris or the use of corrosive solutions.[24] Here, the thermochemical functionalisation method is extended by using a broader range of monomers with intrinsic cationic or anionic functional groups to modify the surface characters of MWCNTs. The goal was to increase the

surface charge on the MWCNTs, using the same set of pre-existing reactive sites, and to simplify the reaction scheme. Additionally, the approach was applied to CB nanoparticles, in order to demonstrate its versatility and to provide panel of CNMs with identical surface chemical properties but different geometry.

2. Results and Discussion

2.1 MWCNTs functionalization

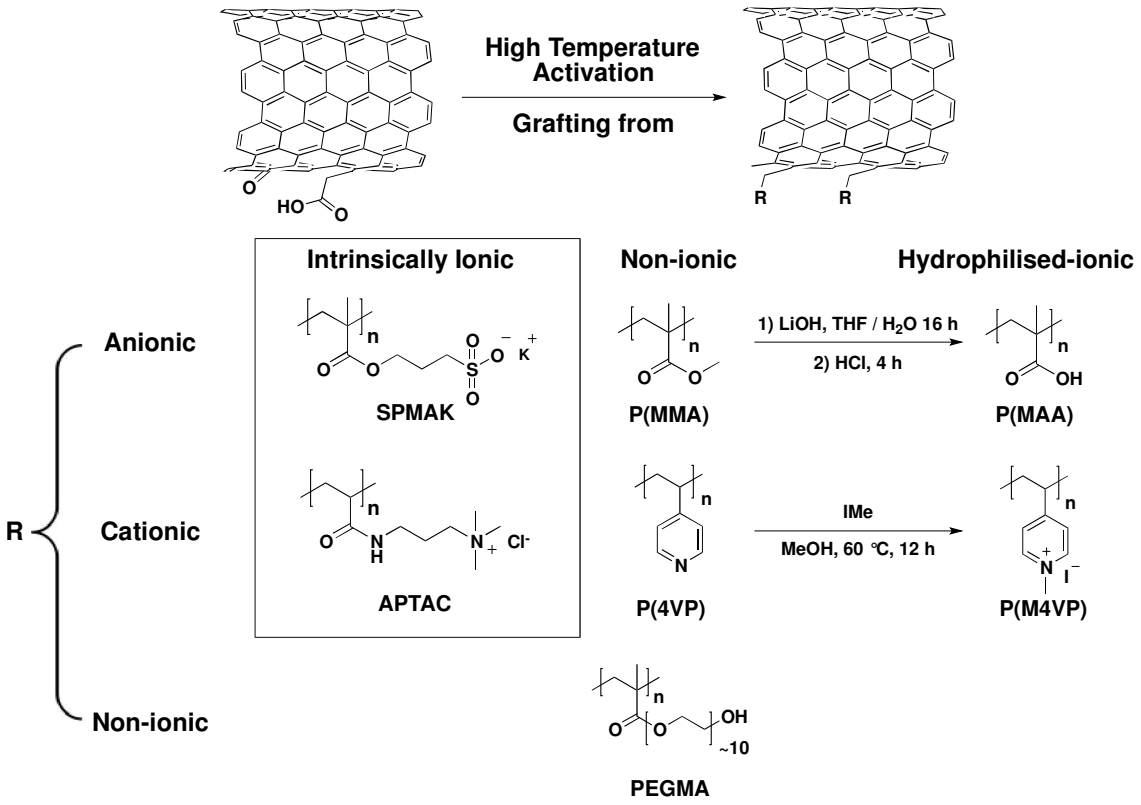

Scheme 1. Reaction scheme for the thermochemical 'grafting from' MWCNTs comparing intrinsically ionic monomers, non-ionic hydrophilic monomers (PEGMA), and non-ionic monomers (MMA and 4VP) that can be hydrophilised by subsequent reaction to form ionic species (MAA and M4VP respectively).

In the previous study, a thermochemical approach was successfully applied for preparation of a panel of cationic, anionic and non-ionic functionalized-MWCNTs (*f*-MWCNTs), via the modification of the initially uncharged grafted oligomers, by hydrolysis or quaternisation. Specifically, poly(methyl methacrylate) (PMMA) was hydrolysed to poly(methacrylic acid) (P(MAA)), N-methyl 4-vinylpyridine iodide (M4VP) was obtained by methylation of 4-vinylpyridine (4VP); and non-ionic poly (ethylene glycol) methacrylate (PEGMA) monomer was grafted as a bulky side chain acrylate

(reactions shown in Scheme 1). The *f*-MWCNTs retained their carbon framework and displayed significantly enhanced water compatibility.[24,25] In order to simplify the synthesis process and further increase the magnitude of surface charge (and hence the colloidal stability of the system), two intrinsically ionic monomers, 3-sulfopropyl methacrylate potassium salt (SPMAK) and (3-acrylamidopropyl) trimethylammonium chloride (APTAC), with explicit anionic and cationic functional groups on the backbone respectively, were employed to modify the surface characteristics of MWCNTs using the same thermochemical mechanism (refer to Scheme 1).

2.1.1 Characterisation of the *f*-MWCNTs

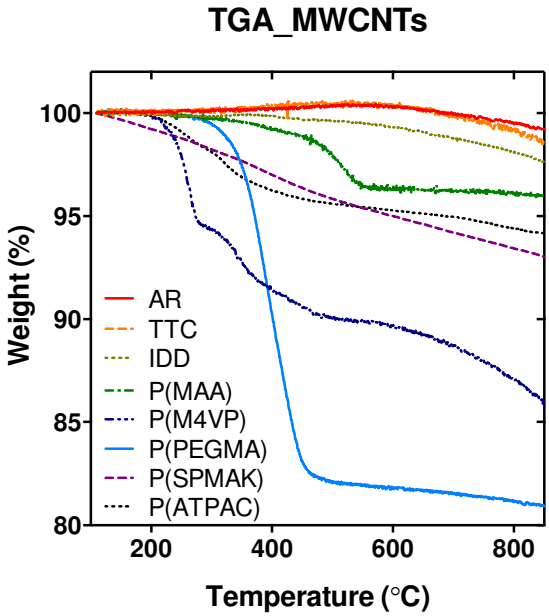

Figure 1. TGA weight loss profiles of as-received (AR) MWCNTs, thermal treated control (TTC) MWCNTs and various *f*-MWCNTs, heated in N_2 atmosphere with a 10 ℃/min ramping rate from 100 ℃ to 850 ℃. Note that TGA curves and other data within this paper regarding P(MAA), P(M4VP), P(PEGMA), IDD grafted MWCNTs have been adapted from our previous report.[25]

Table 1. Grafting ratios deduced from weight loss, wt% (weight percentage of grafted oligomers in total grafted sample weight), grafting concentration (moles of monomer per gram of MWCNTs), and estimated degree of polymerisation (number of repeating monomeric units). The table summarises the results for the new reagents and those previously reported,[25] calculated based on TGA profiles (Figure 1).

Sample Code	Grafted Compound (chemical name)	M_w	Grafting Ratio (wt%)	Grafting Concentration (μmol/g)	Monomer Repeats
P(SPMAK)-MWCNTs	3-Sulfopropyl methacrylate potassium salt	206.7	9.2	490.2	5.8
P(APTAC)-MWCNTs	(3-Acrylamidopropyl) trimethyl ammonium chloride	246.3	5.0	213.7	2.5
P(MAA)-MWCNTs	Methacrylic acid	86.1	3.4	408.8	4.9
P(M4VP)-MWCNTs	N-methyl 4-vinylpyridine iodide	247.1	8.7	385.6	4.6
P(PEGMA)-MWCNTs	Poly (ethylene glycol) methacrylate	528.9	18.3	423.5	5.0
IDD-MWCNTs	1-Iodododecane	169.3	1.4	83.9	1.0

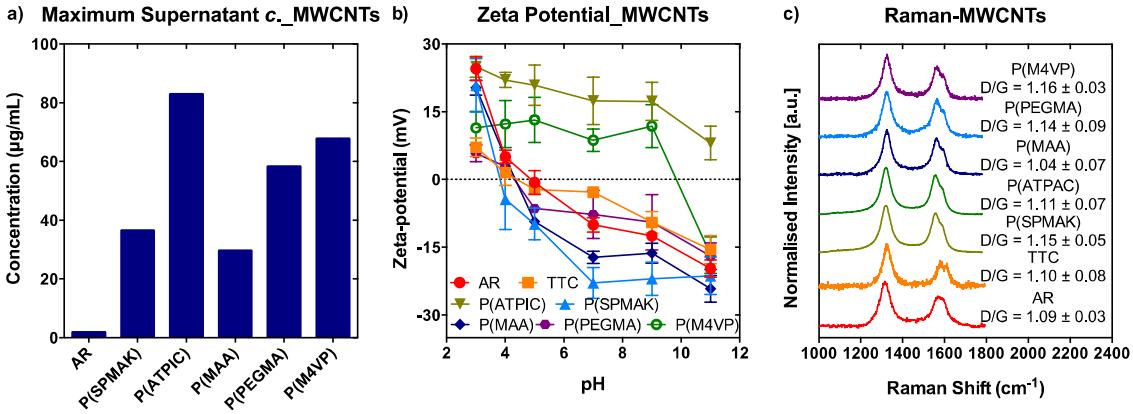

Figure 2. a) The supernatant concentrations of various *f*-MWCNTs were quantitatively determined by UV absorbance with a loading concentration of 2 mg/mL; b) zeta-potential analysis of AR, TTC and *f*-MWCNTs as a function of pH. Error bars are mean ± standard deviation (SD) (n = 5) c) Raman spectroscopy analysis of AR, TTC and *f*-MWCNTs.

Table 2. Maximum supernatant concentration (with loading concentration 2 mg/mL), zeta-potential in pH 7 HPLC water, isoelectric point (IEP) and D / G ratio of AR and grafted MWCNTs.

Sample Code	Maximum supernatant concentration in water (µg/mL)	Zeta-potential (mV) in pH 7 HPLC water	IEP	D/G Ratio
P(SPMAK)-MWCNTs	36.5	-22.9 ± 3.4	3.8	1.11 ± 0.07
P(APTIC)-MWCNTs	82.9	19.2 ± 1.4	N/A	1.15 ± 0.05
P(MAA)-MWCNTs	29.6	-17.2 ± 1.3	4.3	1.03 ± 0.07
P(PEGMA)-MWCNTs	58.3	-7.8 ± 5.3	4.6	1.13 ± 0.09
P(M4VP)-MWCNTs	67.8	8.7 ± 2.4	9.8	1.04 ± 0.03

The grafting ratios and degrees of polymerisation of the new ionic monomers were characterised based on TGA analysis (Figure 1, Table 1). In contrast to as-received (AR) and non-grafted thermal treated control (TTC) MWCNTs, significant weight losses occurred for the *f*-MWCNTs, which are attributed to the decomposition of the grafted organic oligomers/polymers. This step indicates that successful oligomer/polymer grafting has been achieved. The grafting ratio was calculated based on the difference between the weight percentage of *f*-MWCNTs and TTC-MWCNTs, in order to exclude any effect of minor volatile/absorbed impurities within the AR-MWCNTs. The TTC sample was obtained using the same activation protocol as functionalisation, but exposing activated MWCNTs to air rather than a monomer, at ambient temperatures.[24,25] In order to estimate the number of active sites, the MWCNTs were grafted with the non-polymerisable reagent 1-iododododecane (IDD).[25] A

154 further control of treating TTC-MWCNTs with monomer MMA, followed by standard
155 workup, indicated that unreacted monomer was completely removed; thus simple
156 physisorption of monomers on MWCNTs does not contribute to the grafting ratios
157 obtained (Figure S1).
158 The negatively charged P(SPMAK)-MWCNTs have a grafting ratio of 9.2 wt% with a
159 calculated repeating monomeric unit of 5.8, similar to the previously reported anionic
160 P(MAA)-MWCNTs (Table 1). The two types of anionically charged MWCNTs
161 displayed similar decreasing trends in their zeta-potential curves on increasing
162 solution pH due to the protonation/deprotonation of either sulfonyl or carboxylic acid
163 groups. The P(SPMAK)-MWCNTs displayed a lowered IEP at 3.8 compared to
164 P(MAA)-MWCNTs at 4.3, as expected qualitatively from the relative pK_a values of the
165 respective acids. In addition, a more negative zeta-potential in pH 7 aqueous solution
166 was obtained (-22.9 mV) for P(SPMAK)-MWNTs than P(MAA)-MWCNTs (-17.2 mV),
167 presumably due to the higher grafted concentration. As a result, P(SPMAK)-MWCNTs
168 showed even better water compatibility, with a 23 % improvement of water solubility
169 compared to P(MAA)-MWCNTs, as measured by UV analysis.
170 The positively charged P(APTAC)-MWCNTs displayed a 5.0 wt% grafting ratio with a
171 low monomer repeat of only 2.5. Although the grafting concentration and number of
172 monomeric repeats were lower than the other types of *f*-MWCNTs, the water
173 dispersibility of P(ATPAC)-MWCNTs was still improved compared to the positively
174 charged P(M4VP)-MWCNTs. The aqueous dispersion of P(ATPAC)-MWCNTs
175 displayed the highest concentration of 82.9 μg/mL within the f-MWCNTs panel. Again,
176 the surface charge properties were quantified by zeta-potential analysis. The results
177 showed that the P(ATPAC)-MWCNTs sample retained a positive zeta-potential in
178 aqueous solutions even up to pH 11. In pH 7 aqueous solution, the zeta-potential of

P(ATPAC)-MWCNTs was + 19.2 mV, much improved compared to P(M4VP)-MWCNTs (+ 8.7 mV).

The new ionic monomer grafted MWNTs appeared undamaged by the process, as anticipated, semi-quantitatively confirmed by the unchanged, D/G ratio characterized by Raman spectroscopy (Figure 2c, Table 2).

2.2 Carbon black NP functionalisation

As mentioned earlier, the thermochemical functionalisation approach has great potential to be applied to other types of CNMs, as the surface chemistry is expected to be similar. CNMs produced by gas phase processes, in particular, may be expected to have a similar set of defective surface sites that can be converted to active radicals. As a proof of such a concept, CB was selected as a case study to investigate the versatility of the method. Although likely more defective, CB nanoparticles are chemically related, especially to CVD MWCNTs, and hence can provide an interesting control system for the panel of *f*-MWCNTs, with a different geometry.

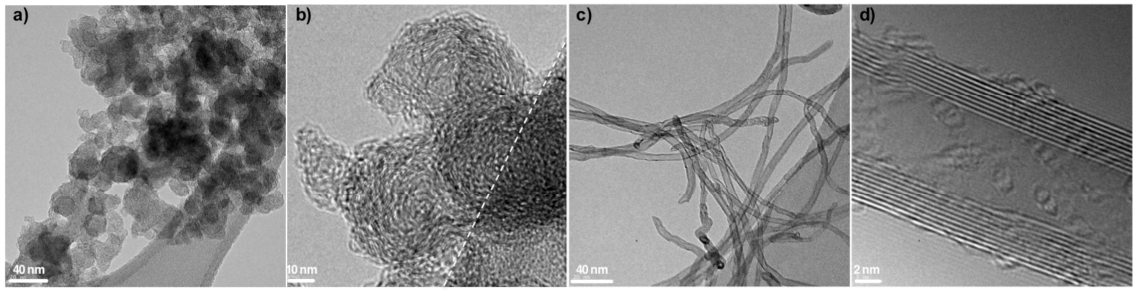

Figure 3. a,c) Low resolution and b,d) high resolution bright field TEM images showing the morphology and crystallinity of CB (a,b) nanoparticles and MWCNTs (c,d). The white dashed line in 3b indicates the edge of the underlying amorphous carbon film of the TEM grid.

As shown in Figure 3b, AR-CB displayed layered carbon-sheet structures, but with much lower crystallinity than the MWCNTs (Figure 3d). The CB nanoparticles employed in this study had an average primary particle diameter of 21.1 ± 6.2 nm (N=100), as determined by analysis of LR-TEM images (Figure 3a), which is only slightly larger than that of the MWCNTs used whose average diameter is 12.1 ± 3.7 nm (N=100). Given the similarities in chemical components, diameter and other properties (which will be further discussed below), the two materials can provide interesting comparisons to study geometric effects systematically.

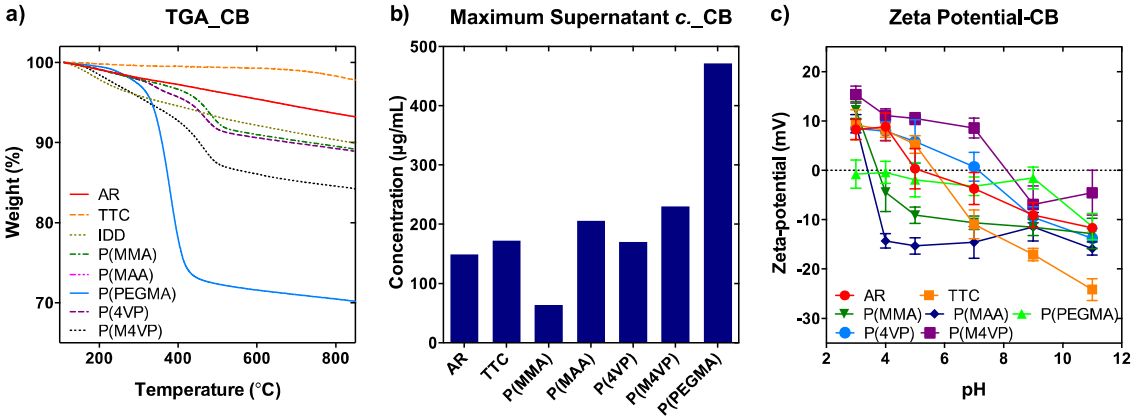

Figure 4. a) TGA weight loss profiles of as-received (AR) CB, thermally treated control (TTC) CB and various functionalised CB (*f*-CB), heated in N_2 atmosphere with a 10 ℃/min ramp rate from 100 to 850 ℃; b) the supernatant concentrations of various *f*-CB were quantitatively determined by UV absorbance with a loading concentration of 2 mg/mL; c) zeta-potential analysis of AR, TTC and *f*-CB as a function of pH. Error bars are mean ± standard deviation (SD) (n = 5)

Table 3. Grafting ratios in weight loss, wt% (weight percentage of grafted oligomers in total grafted sample weight), grafting concentration (moles of monomer per gram of CB), and estimated degree of polymerisation (number of monomer repeats), calculated based on TGA profiles (Figure 4b); maximum supernatant concentration (with loading concentration 2 mg/mL), zeta-potential in pH 7 HPLC water, isoelectric point (IEP) and D/G ratio of AR and *f*-CB.

Sample Code	Grafting Ratio (wt%)	Grafting Concentration (µmol/g)	Monomeric Repeats	Solubility in water (µg/mL)	Zeta-potential (mV) in pH 7 HPLC water	IEP
AR-CB	N/A	N/A	N/A	149.0	-3.7 ± 3.2	5.0
TTC-CB	N/A	N/A	N/A	172.1	-11.0 ± 2.9	5.6
P(MMA)-CB	8.6	940.0	1.9	63.9	-10.6 ± 1.4	3.8
P(MAA)-CB	5.9	728.2	1.4	205.9	-14.6± 3.2	3.4
P(4-VP)-CB	8.9	929.5	1.8	170.0	0.7 ± 3.0	7.0
P(M4VP)-CB	13.6	637.0	1.3	230.2	8.6 ± 2.0	8.1
P(PEGMA)-CB	27.6	720.8	1.4	465.8	-3.3 ± 1.9	N/A
IDD-CB	7.9	506.7	1.0	N/A	N/A	N/A

Using an identical preparation process as described above, anionic CB (P(MAA)-CB) were obtained by hydrolysis of hydrophobic methyl methacrylate grafted CB in alkaline solution. The weak base P(4-VP)[26] was quaternised using iodomethane (IMe) to obtain more stable aqueous dispersions of protonated polymer (P(M4VP)) grafted CB. TGA analysis confirmed the successful grafting of CB nanoparticles. The TGA profile of AR-CB displayed continuous weight loss between 100 to 850 ℃, due to the lower thermal stability of less crystalline carbon framework compared to MWCNTs. In contrast to as-received (AR) and non-grafted thermal treated control (TTC) CB, a

second range of significant weight loss occurred around 200-500 ℃ for *f*-CB, which is attributed to the decomposition of the grafted organic oligomers/polymers. This step indicates successful oligomer/polymer grafting.

The grafting ratio of the P(MMA)-CB (8.6 wt%) decreased slightly after the hydrolysis treatment (5.9 wt%), due to the loss of methyl groups. The grafting ratio of 4-VP-grafted CB was 8.9 wt%, and the degree of polymerisation was very similar to that of the P(MMA)-CB. TGA of the quaternised product retained the features of the P(4-VP)-CB, associated with the combustion of the grafted oligomer, with additional weight loss (4.7%) between 100 to 300 ℃, attributed to the methyl group and the associated iodide counter-ion. The higher grafting ratio of P(PEGMA) grafted CB, 27.6 wt%, is partly attributed to the high molecular weight of side chain of PEGMA monomer (Table 3).

Compared to previously reported *f*-MWCNTs, the cationic (M4VP), anionic (MAA) and non-ionic (PEGMA) grafted CB samples displayed a similar trend of grafting ratio, namely P(PEGMA)>P(M4VP)>P(MAA).

Table 4. Comparisons of IDD grafted CB and MWCNTs[25] in terms of grafting ratios in weight loss, wt% (weight percentage of grafted oligomers in total grafted sample weight), grafting concentration (moles of IDD in per gram of CNMs), BET surface area, and another estimated grafting concentration (moles of IDD per m^2 of carbon surface.

Sample Code	Grafting Ratio (wt%)	Grafting Concentration (μmol/g)	BET surface area (m^2/g)	Grafting Concentration (μmol/m^2)
IDD-CB	7.9	506.7	270	1.88
IDD-MWCNTs	1.4	84.1	227	0.37

Based on grafting ratios of the non-polymerisable reagent IDD, the reactive site concentrations on CB and MWCNTs can be compared. As might be expected from the more defective structure, the number of active sites identified was higher on the CB (approximately 1 per 200 carbons) than MWCNTs (1 per 1000), both by mass and when normalised to surface area (Table 3). However, the cationic (M4VP), anionic (MAA) and non-ionic (PEGMA) grafted CB did not show a significant increase in the total grafting ratios compared to the MWCNTs grafted with the same monomers. Instead, the apparent number of monomer repeats was consistently reduced. One possible explanation is that the higher density of radicals on the CB surface not only increased the number of polymerisation initiation sites, but also the rate of termination of the polymerization. Termination may either occur by reaction between two short oligomers or the quenching of a growing oligomer by a nearby radical site. It is worth mentioning that in this study, the grafting density and degree of polymerisation are estimated assuming that IDD reacts stoichiometrically with all active radical sites and the polymerisation processes is initiated at a radical site but can terminate anywhere on the CB or MWNT surface; in other words that each oligomer/polymer chain consumes one radical site.[25] However, if chain-chain or chain-radical site termination dominates, each chain would be associated with two radical sites in total; implementing this assumption would lead to doubled values for estimated chain length (monomer repeats) and halved grafting concentrations per unit area. These two

alternative estimates represent limits for the true average value. However, a further complication is that the active radical sites on the carbon surface may be not equally accessible to the IDD probe and the monomers used. If steric effects are significant and the monomers are more bulky, then again the real chain length will be longer and the grafting density lower, than currently estimated. This effect may be more significant, for the high defect density CBs. Further work on mechanism is needed; current experiments are exploring the use alkyl iodides with different chain lengths, to explore the influence of steric constraints.

The water solubility of AR and *f*-CB samples has been quantified by UV-vis analysis. Due to the high density of oxygen-containing functional groups on CB surfaces, the AR-CB sample already has a moderately high water solubility of 149 µg/mL. After functionalisation, *f*-CB, stablised by cationic, anionic and non-ionic charges displayed further improved water dispersibility, reaching 230, 206 and 472 µg/mL respectively. The higher concentration obtained for P(PEGMA) grafted CB can be attributed to high steric stabilisation effect of PEG chains and the much higher grafting ratio than cationic and anionic CB.

The zeta potential analysis further confirmed successful grafting of the CB with anionic, non-ionic and cationic oligomers/polymers (Figure 4c). The AR-CB and TTC-CB are weakly acidic, with an iso-electric point (IEP) of 5.0 and 5.6, as expected given the surface oxides, including carboxylic acid groups, present on the CB surface. The lowered IEP at 3.4 for P(MAA)-CB compared to P(MMA)-CB (IEP 3.8), confirmed the successful hydrolysis process. Moreover, the improved plateau voltage value of P(MAA)-CB (~ -15 mV) from P(MMA)-CB (~ -10 mV), again, provided proof of successful reaction. The 4-VP functionalised systems introduce positively-charged groups, shifting the IEP to higher pH; by introducing a positive charge through

quaternisation, the IEP of P(M4VP)-CB was successfully increased to about pH 8.1. The grafted PEGMA is non-ionic and the zeta potential of aqueous dispersions (up to pH 9) of P(PEGMA)-CB samples remain close to zero, indicating that the original acidic surface oxides are indeed activated and converted to non-ionic PEG-based chains.

3. Experimental methods

3.1 Materials

MWCNTs (diameter 12.1 nm, s.d. 3.7 nm), synthesised by CVD, were obtained from Arkema SA (Lacq-Mourenx, France). Carbon black nanoparticles (Printex 90, primary particle diameter 21.1 nm, s.d. 6.2 nm) were provided by Degussa-Hüls (Frankfurt, Germany). Potassium 3-(methacryloyloxy)propane-1-sulfonate (SPMAK, 98%), (3-acrylamidopropyl)trimethylammonium chloride solution (75% in H_2O), methyl methacrylate (MMA, > 98.5%), 4-vinyl pyridine (4-VP, 95%), poly(ethylene glycol) methacrylate (PEGMA, average $M_n = 530$), 1-iodododecane (IDD, 98%), iodomethane (IMe, ≥ 99%), and lithium hydroxide (LiOH, 98%) were purchased from Sigma-Aldrich for CNM functionalisation. Before use, all liquid monomer chemicals were passed through a chromatographic column consisting of neutral and basic aluminium oxide powders (aluminium oxide 90 (0.063-0.200 mm), activity stage I for column chromatography, Merck Millipore, Germany) and further degassed by bubbling N_2 gas for at least 30 minutes, in order to remove any radical inhibitors and oxygen.

3.2 Functionalisation of CNM

3.2.1 Thermochemical grafting

The thermal activation process was carried out in a custom-made 30 mm diameter quartz tube attached to a sample flask, and the whole setup was connected to a vacuum system. In a typical experiment, 100 mg of CNM were heated to 1000 ℃ at a constant ramping rate of 15 ℃/min under vacuum (~ 5×10^{-4} mbar), in a three-zone tube furnace (PTF 12/38/500, Lenton Ltd, UK) and held at the activation temperature for 2 hours. After the activation step, the quartz tube was slowly removed from the heating zone and allowed to cool to room temperature under vacuum. The CNM were

then transferred to the connected round bottom flask by gravity. 8 mL of the reactant (for SPMAK, 1 g of compound was dissolved in degassed 1:1 v/v ethanol H_2O co-solvent) was then injected into the flask containing the thermally-activated CNM. The reaction mixture was stirred at room temperature overnight. The unreacted reactant was removed via filtration through a 0.10 or 0.45 μm pore size polytetrafluoroethylene (PTFE) membrane (Whatman, UK) under vacuum. The product was thoroughly washed with 3 × 90 mL of washing solvent (details of which solvent to be used for each grafting reagent can be found in ESI), then dispersed in 90 mL of solvent and bath sonicated (USC300T, 45kHz, 80W, VWR International, USA) for 15 minutes. The filtration-sonication cycle was repeated three times in order to remove any physically absorbed reactants. The functionalised CNM are named by the abbreviation of the grafted polymer and CNM type: e.g. P(SPMAK)-MWCNTs. The other sample codes can be found in Table 1.

3.2.2 Post-functionalisation of *f*-CB

3.2.2.1 Synthesis of P(M4VP)-CB

P(4-VP)-CB (20 mg) were dispersed in 10 mL of methanol (99.8%, Sigma-Aldrich) by sonication for 5 minutes; IMe (3.12 mL, 50.0 mmol) was added drop-wise, and the reaction mixture was heated to 60 ℃ overnight under N_2 atmosphere.[27] Afterwards, the mixture was cooled to room temperature and filtered through a 0.10 μm PTFE membrane. The CB were washed with 3 × 30 mL of ethanol, then dispersed in 30 mL of ethanol and bath sonicated for 15 minutes. The filtration-sonication cycle was repeated three times in order to remove any physically absorbed reactants.

3.2.2.2 Synthesis of P(MAA)-CB

LiOH (40 mg) was dissolved in 20 mL 10:1 v/v THF/water co-solvent before adding 20 mg of P(MMA)-CB. The reaction mixture was bath sonicated for 5 min to obtain a

good dispersion, and then stirred at room temperature overnight. Subsequently, 37% hydrochloric acid (HCl, AnalaR grade, BDH) was added drop-wise until the pH value of the solution reached pH 2.[28] The mixture was stirred for another 12 hours, then filtered on a 0.10 µm PTFE membrane, and washed with water (3 × 30 mL). The CB residue was dispersed in 30 mL of water by bath sonication for 15 minutes. The filtration-sonication cycle was repeated three times in order to remove any remaining salt and acid.

3.3 Characterisation of CNM

3.3.1 Thermogravimetric analysis (TGA)

TGA analyses were carried out using a Perkin Elmer Pyris 1, by heating 1.8 ± 0.2 mg CNM samples to 100 °C, under a N_2 atmosphere (60 mL/min), and holding isothermally for 30 minutes to remove residual water and/or solvent; the temperature was then increased from 100 to 850 °C at a constant ramping rate of 10 °C/min under flowing N_2 (60 mL/min).

3.3.2 Zeta-potential measurement

Zeta-potential analyses were performed on a Brookhaven ZetaPALS. *f*-CNMs samples were dispersed in HPLC water with a concentration of 50 µg/mL by bath sonication for 15 minutes. The pH was adjusted using 0.1 or 0.01 M HCl/NaOH, measured by a digital pH meter (VWR sympHony™ meter, VWR International, USA).

3.3.3 Raman spectroscopy

Raman spectra (1000 – 1800 cm^{-1}) were collected on a LabRam Infinity Raman spectrometer, using a 532 nm laser (scan time 90 s, average 3 scan cycles). The D/G ratio was determined from the ratio of integrated intensity under the Raman bands at

around 1350 cm^{-1} (D-band) and 1580 cm^{-1} (G-band) respectively.[29] Average values and standard deviations were obtained from five independent measurements.

3.3.4 UV–vis spectroscopy

The water compatibility of *f*-CNMs was quantified by UV-vis spectroscopy (Lambda 950, Perkin Elmer). For water solubility tests, as-received and *f*-CNMs were bath sonicated (45 kHz, 80 W, VWR International, USA) in HPLC water for 15 minutes with different initial powder loading concentrations of 2 mg/mL.CNM aggregates were settled by centrifugation for 15 minutes at 10, 000 g. The supernatant was carefully decanted and the concentration of grafted MWCNTs determined by UV absorbance and application of the Beer-Lambert law, $A = \varepsilon \times c \times d$, where A is the measured UV absorbance, ε is the extinction coefficient (35.10 mL/mg/cm for Arkema MWCNTs at 800 nm,[30] 19.45 mL/mg/cm for CB nanoparticles at 800 nm) and d is the light path length (1 cm cuvette length, in this study).

3.3.5 Specific surface areas

The measurements of adsorption and desorption isotherms of nitrogen at 77 K were carried out on 100 mg CNMs using a Micromeritics ASAP 2010 apparatus. Specific surface areas were calculated according to the Brunauer, Emmet and Teller (BET) equation from the adsorption isotherm in the relative pressure range of 0.05-0.20 p/p_0.

4. Conclusion

In this paper, MWCNTs have been successfully grafted with new, intrinsically ionic positive and negative monomers using a thermochemical approach, leading to aqueous dispersions of f-MWCNTs with increased surface charge and enhanced water dispersibility compared to previously published results. The degree of functionalisation is quantified by TGA analysis, and a combination of UV-vis and zeta-potential techniques confirm the altered surface charge and water compatibility of the panel of *f*-MWCNTs. Further, the thermochemical method was also been successfully applied to another important class of CNMs, specifically carbon black (CB). Again, the TGA, UV-vis, and zeta-potential analyses confirmed successful grafting and water compatibilisation.

Building on previous work, these charged MWCNTs can serve as model materials, which can be delivered in aqueous conditions, for cytotoxicity and cell uptake investigations; the new monomer systems offer simplified preparation protocols and further improved water solubility. The *f*-CB samples, with closely matched surface chemical properties, provide excellent controls for the toxicity tests using in vitro cell models, for exploring geometric effects, and are under investigation. In addition, water dispersible CNMs are desirable in a wide range of applications, from printing conductive inks, to assembling filters and electrodes. The versatility of the functionalisation route presented, to address both different classes of carbons and different types of surface grafting, whilst minimizing carbon framework damage, is very attractive. Pure gas phase embodiments of the process avoid time-consuming filtration steps, minimize waste, and are readily scalable. Current investigations are exploring the modification of other types of carbon nanomaterials, including single-walled

carbon nanotubes, MWCNTs grafted carbon fibres,[31] carbon aerogels, and graphene, as well fundamental aspects of the carbon surface chemistry. The potential applications of such materials will be explored and may be extended by including functional components, for example, pseudocapacitive groups for supercapacitors or metal[24]/oxide[32] catalyst binding groups for heterogeneous reactions.

Acknowledgements

The authors would like to thank NIEHS (grant# U19ES019536) for the funding of this project. AP acknowledges an individual ERC starting grant for additional funding for SC and ADG (project number: #257182). MSPS/RM acknowledge the Engineering and Physical Sciences Research Council (EPSRC) for additional financial support (grant# EP/G007314/1). However, the views expressed in this paper are solely of the authors and do not necessarily reflect those of the funding agencies.

5. Reference:

1. Y. Gogotsi and V. Presser, *Carbon nanomaterials*, CRC Press, 2013.
2. X. Wang, C. Wang, L. Cheng, S.-T. Lee, and Z. Liu, *J. Am. Chem. Soc.*, 2012, **134**, 7414–7422.
3. K. Yang, L. Hu, X. Ma, S. Ye, L. Cheng, X. Shi, C. Li, Y. Li, and Z. Liu, *Adv. Mater.*, 2012, **24**, 1868–1872.
4. A. A. Bhirde, V. Patel, J. Gavard, G. Zhang, A. A. Sousa, A. Masedunskas, R. D. Leapman, R. Weigert, J. S. Gutkind, and J. F. Rusling, *ACS Nano*, 2009, **3**, 307–316.
5. M. Chen, Y. He, X. Chen, and J. Wang, *Bioconjugate Chem.*, 2013, **24**, 387–397.
6. A. de la Zerda, Z. Liu, S. Bodapati, R. Teed, S. Vaithilingam, B. T. Khuri-Yakub, X. Chen, H. Dai, and S. S. Gambhir, *Nano Lett.*, 2010, **10**, 2168–2172.
7. L. G. Delogu, G. Vidili, E. Venturelli, C. Ménard-Moyon, M. A. Zoroddu, G. Pilo, P. Nicolussi, C. Ligios, D. Bedognetti, F. Sgarrella, R. Manetti, and A. Bianco, *P Natl Acad Sci. U.S.A.*, 2012, **109**, 16612–16617.
8. N. Karousis, N. Tagmatarchis, and D. Tasis, *Chem. Rev.*, 2010, **110**, 5366–5397.
9. V. Georgakilas, M. Otyepka, A. B. Bourlinos, V. Chandra, N. Kim, K. C. Kemp, P. Hobza, R. Zboril, and K. S. Kim, *Chem. Rev.*, 2012, **112**, 6156–6214.
10. S. W. Kim, T. Kim, Y. S. Kim, H. S. Choi, H. J. Lim, S. J. Yang, and C. R. Park, *Carbon*, 2012, **50**, 3–33.
11. Y. Wang, Z. Iqbal, and S. Mitra, *J. Am. Chem. Soc.*, 2006, **128**, 95–99.
12. M. Shaffer, X. Fan, and A. H. Windle, *Carbon*, 1998, **36**, 1603–1612.
13. J. M. Gónzalez-Dominguez, M. Gonzalez, A. Anson-Casaos, A. M. Diez-Pascual, M. A. Gomez, and M. T. Martinez, *J. Phys. Chem. Lett.*, 2011, **115**, 7238–7248.
14. K. Li, C. Zhang, Z. Du, H. Li, and W. Zou, *Synth. Met.*, 2012, **162**, 2010–2015.
15. M. N. Tchoul, W. T. Ford, G. Lolli, D. E. Resasco, and S. Arepalli, *Chem. Mater.*, 2007, **19**, 5765–5772.
16. V. Datsyuk, M. Kalyva, K. Papagelis, J. Parthenios, D. Tasis, A. Siokou, I. Kallitsis, and C. Galiotis, *Carbon*, 2008, **46**, 833–840.
17. I. Mazov, V. L. Kuznetsov, and I. A. Simonova, *Applied Surface Science*, 2012, **258**, 6272-6280.
18. Y. Zhu, S. Murali, W. Cai, X. Li, J. W. Suk, J. R. Potts, and R. S. Ruoff, *Adv. Mater.*, 2010, **22**, 3906–3924.
19. S. Fogden, R. Verdejo, B. Cottam, and M. Shaffer, *Chem. Phys. Lett.*, 2008, **460**, 162–167.
20. J. P. Rourke, P. A. Pandey, J. J. Moore, M. Bates, I. A. Kinloch, R. J. Young, and N. R. Wilson, *Angew. Chem. Int. Ed.*, 2011, **50**, 3173–3177.
21. S. Banerjee, T. Hemraj Benny, and S. S. Wong, *Adv. Mater.*, 2005, **17**, 17–29.
22. M. Tunckol, S. Fantini, F. Malbosc, J. Durand, and P. Serp, *Carbon*, 2013, **57**, 209–216.

23. Y. Zhao and J. F. Stoddart, *Acc. Chem. Res.*, 2009, **42**, 1161–1171.
24. R. Menzel, M. Q. Tran, A. Menner, C. Kay, A. Bismarck, and M. S. P. Shaffer, *Chem. Sci.*, 2010, **1**, 603–608.
25. S. Chen, S. Hu, E. F. Smith, P. Ruenraroengsak, A. J. Thorley, R. Menzel, A. E. Goode, M. P. Ryan, T. D. Tetley, A. E. Porter, and M. S. P. Shaffer, *Biomaterials*, 2014, **35**, 4729–4738.
26. L. Franck-Lacaze, P. Sistat, and P. Huguet, *J. Membrane. Sci.*, 2009, **326**, 650–658.
27. S. Alunni, V. Laureti, L. Ottavi, and R. Ruzziconi, *J. Org. Chem.*, 2003, **68**, 718–725.
28. S. P. Runyon, L. E. Brieaddy, S. W. Mascarella, J. B. Thomas, H. A. Navarro, J. L. Howard, G. T. Pollard, and F. I. Carroll, *J. Med. Chem.*, 2010, **53**, 5290–5301.
29. M. S. Dresselhaus, G. Dresselhaus, R. Saito, and A. Jorio, *Phys. Rep.,* 2005, **409**, 47–49.
30. M. Q. Tran, C. Tridech, A. Alfrey, A. Bismarck, and M. Shaffer, *Carbon*, 2007, **45**, 2341–2350.
31. H. Qian, A. Bismarck, E. S. Greenhalgh, and M. S. P. Shaffer, *Compos. Sci. Technol.*, 2010, **70**, 393–399.
32. A. Garcia-Gallastegui, D. Iruretagoyena, M. Mokhtar, A. M. Asiri, S. N. Basahel, S. A. Al-Thabaiti, A. O. Alyoubi, D. Chadwick, and M. S. P. Shaffer, *J. Mater. Chem.*, 2012, **22**, 13932–13940.